

Chapter 3 Landing Gear Concept Selection

3.1. Introduction

The design and positioning of the landing gear are determined by the unique characteristics associated with each aircraft, *i.e.*, geometry, weight, and mission requirements. Given the weight and *cg* range of the aircraft, suitable configurations are identified and reviewed to determine how well they match the airframe structure, flotation, and operational requirements. The essential features, *e.g.*, the number and size of tires and wheels, brakes, and shock absorption mechanism, must be selected in accordance with industry and federal standards discussed in the following chapters before an aircraft design progresses past the concept formulation phase, after which it is often very difficult and expensive to change the design [19]. Three examples of significant changes made after the initial design include the DC-10-30, which added the third main gear to the fuselage, the Airbus A340, where the main gear center bogie increased from two to four wheels in the -400 series, and the Airbus A-300, where the wheels were spread further apart on the bogie to meet LaGuardia Airport flotation limits for US operators.

Based on the design considerations as discussed in this chapter, algorithms were developed to establish constraint boundaries for use in positioning the landing gear, as well as to determine whether the design characteristics violate the specified requirements. The considerations include stability at takeoff/touchdown and during taxiing, braking and steering qualities, gear length, attachment scheme, and ground maneuvers.

3.2. Configuration Selection

The nose wheel tricycle undercarriage has long been the preferred configuration for passenger transports. It leads to a nearly level fuselage and consequently the cabin floor when the aircraft is on the ground. The most attractive feature of this type of undercarriages is the improved stability during braking and ground maneuvers. Under normal landing attitude, the relative location of the main assembly to the aircraft *cg* produces a nose-down pitching moment upon touchdown. This moment helps to reduce the angle of attack of the aircraft and thus the lift generated by the wing. In addition, the braking forces, which act behind the aircraft *cg*, have a stabilizing effect and thus enable the pilot to make full use of the brakes. These factors all contribute to a shorter landing field length requirement.

The primary drawback of the nose wheel tricycle configuration is the restriction placed upon the location where the main landing gear can be attached. With the steady increase in the aircraft takeoff weight, the number of main assembly struts has grown from two to four to accommodate the number of tires required to distribute the weight over a greater area. However, stability and performance constraints as identified by Holloway *et al.* [10] and Sliwa [11] effectively eliminate all but a few locations where the main assembly can be attached. The attachment limitation phenomenon is known as the location stagnation [App. A] and can become a major concern for future large aircraft, where additional tires and struts are required to alleviate the load being applied to the pavement. Typically, a large trailing-edge extension, *i.e.*, the Yehudi,¹ is employed to alleviate at least in part the location stagnation problem. The Yehudi can result in weight and aerodynamic penalties due to local structural reinforcement and increased wetted area, respectively. However, the increased root chord also allows an increase in absolute root thickness for a given *t/c*. This advantage may outweigh other penalties.

3.3. Landing Gear Disposition

The positioning of the landing gear is based primarily on stability considerations during taxiing, liftoff and touchdown, *i.e.*, the aircraft should be in no danger of turning over on its side once it is on the ground. Compliance with this requirement can be determined by examining the takeoff/landing performance characteristics and the relationships between the locations of the landing gear and the aircraft *cg*.

3.3.1. Angles of Pitch and Roll During Takeoff and Landing

The available pitch angle (θ) at liftoff and touchdown must be equal, or preferably exceed, the requirements imposed by performance or flight characteristics. A geometric limitation to the pitch angle is detrimental to the liftoff speed and hence to the takeoff field length. Similarly, a geometric limitation to the roll angle (ϕ) could result in undesirable operational limit under cross-wind landing condition.

¹Apparently known as a “Yehudi”, this inboard trailing edge extension actually first appeared on the Boeing B-29 to solve a fuselage-nacelle interference problem. Douglas used it first on a swept wing transport on the DC-8, and it was not adopted by Boeing until the 707 design went to the -320 model. The name was first used to describe the wind tunnel part that was made on the spot during the wind tunnel test. “Who’s Yehudi” was a running gag on a popular radio show at the time, as well as the name of a popular violinist (letter from Bill Cook, retired Boeing engineer and author of *The Road to the 707*).

For a given aircraft geometry and gear height (h_g), the limit for the takeoff/landing pitch angle follows directly from Fig. 3.1. The roll angle at which the tip of the wing just touches the ground is calculated using the expression [5, p. 350]

$$\tan \phi = \tan \Gamma + \frac{2h_g}{s-t} - \tan \theta \tan \Lambda \quad (3.1)$$

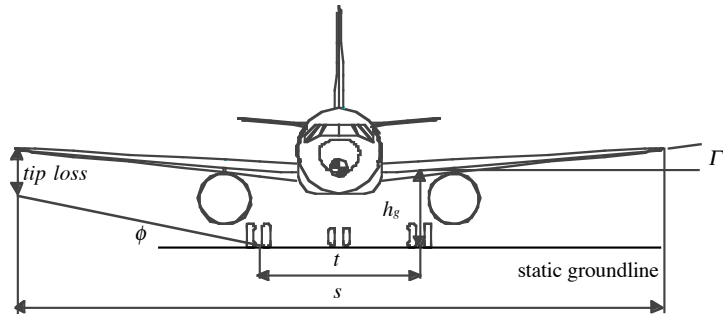
In this case, Γ is taken as the dihedral angle, s is the wing span, t is the wheel track, and Λ is the wing sweep. Similar conditions may be deduced for other parts of the aircraft, except that Γ , Λ and s in Eq. (3.1) must be replaced with appropriate values. For example, the permissible roll angle associated with nacelle-to-ground clearance is determined with the following values: Γ measured from the horizon to the bottom of the nacelle in the front view, Λ measured from the chosen landing gear location to the engine in the top view, and s the distance between the engines.

3.3.1.1. Pitch Angle Required for Liftoff

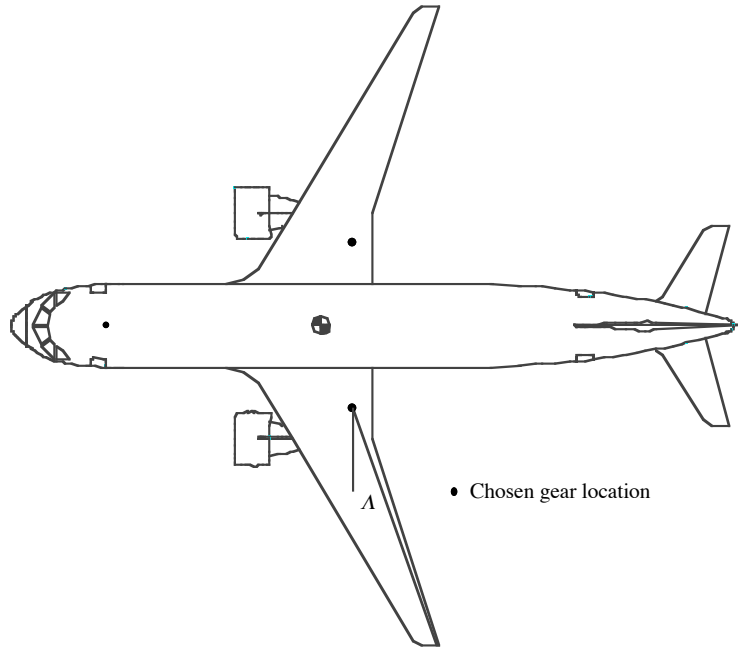
The takeoff rotation angle is prescribed in preliminary design, and then estimated. The final values for θ and ϕ are found as the detailed performance characteristics of the aircraft become available. The pitch angle at liftoff (θ_{LOF}) is calculated using the expression [5, p. 350]

$$\theta_{LOF} = \alpha_{LOF} + \frac{d\theta}{dt} \left(\frac{2l_1}{V_{LOF}} + \sqrt{\frac{l_2}{g} \frac{C_{L_{LOF}}}{dC_L/d\alpha}} \right) \quad (3.2)$$

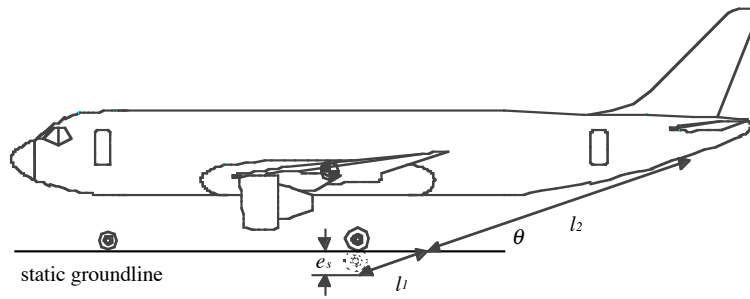
where α_{LOF} is the highest angle of attack anticipated for normal operational use, V_{LOF} is the liftoff speed, g is the gravitational acceleration, $C_{L_{LOF}}$ is the lift coefficient, and $dC_L/d\alpha$ is the lift-curve slope. As shown in Fig. 3.1, the dimension of l_1 and l_2 are defined by the line connecting the tire-ground contact point upon touchdown and the location of the tail bumper, if one is present. For large transports, the typical value for the rate of rotation ($d\theta/dt$) is taken as four degrees per second [5].



a) Front view



b) Top view



c) Side view

Figure 3.1 Geometric definitions in relation to the pitch and roll angles [5]

The detailed aerodynamic data required to use Eq. (3.2) is not always available at the conceptual design stage. In most aircraft the aft-body and/or tail bumper is designed such that the aircraft cannot rotate by more than a specified number of degrees at liftoff. Typically, the value is between 12 and 15 degrees [2]. In addition to the tail scrape problem, the aircraft cg cannot rotate over and aft of the location of the main assembly, a phenomenon known as tail tipping and is critical during landing.

3.3.1.2. *Pitch and Roll Angles During Landing*

With the flaps in the fully-deflected position, the critical angle of attack of the wing during landing is smaller than in takeoff. Consequently, the pitch angle during landing is generally less than that during takeoff. In the absence of detailed information, the pitch angle on touchdown (θ_{TD}) may be assumed equal to θ_{LOF} . As for the roll angle upon touchdown, an upper limit of between five [20] and eight [5] degrees is generally applied to large transport aircraft.

3.3.2. *Stability at Touchdown and During Taxiing*

Static stability of an aircraft at touchdown and during taxiing can be determined by examining the location of the applied forces and the triangle formed by connecting the attachment locations of the nose and main assemblies. Whenever the resultant of air and mass forces intersects the ground at a point outside this triangle, the ground will not be able to exert a reaction force which prevents the aircraft from falling over. As a result, the aircraft will cant over about the side of the triangle that is closest to the resultant force/ground intersect.

Assuming first that the location of the nose assembly is fixed, the lower limit of the track of the landing gear, identified as constraint I in Fig. 3.2, is defined by the line passing through the center of the nose assembly and tangential to the circle with a radius of 0.54 times the height of the aircraft cg (h_{cg}) from the static groundline, centered at the fore-most cg location [5]. The constant 0.54 is based on static and dynamic instability considerations at touchdown and during taxiing. Conversely, if the location of the main assembly is assumed to be fixed, the aft-most limit of the nose assembly mounting

location, identified as constraint II in Fig. 3.2, is defined as the intersection of the aircraft centerline and the line that passes through the center of the main assembly, tangential to the circle with a radius of 0.54 times of the height of aircraft cg .

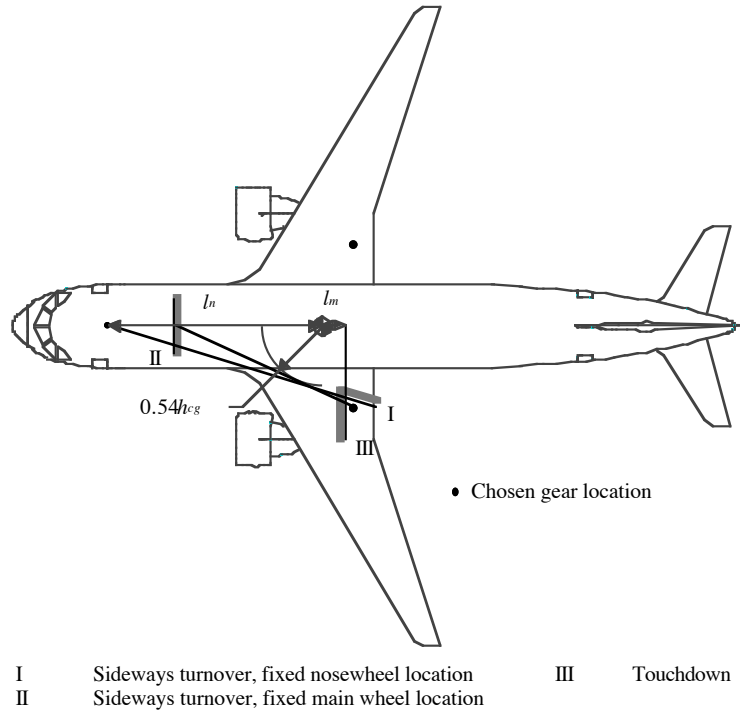


Figure 3.2 Limits for the undercarriage disposition based on stability [5]

3.3.2.1. Condition at Touchdown

The most unfavorable condition at touchdown would be a landing with the aircraft cg at its aft-most and highest location, which can lead to the tail scrape and tail tipping phenomenon mentioned previously. Assuming there are no retarding forces, *i.e.*, spin-up load, a vertical force acting at a distance behind the aircraft cg is needed to produce a moment that will pitch the nose downward. Thus, the minimum allowable offset between the aft-most cg and the main assembly mounting locations, identified as constraint III in Fig. 3.2, is determined using the following expression [5, p. 352]

$$l_m \geq (h_{cg} + e_s) \tan \theta_{TD} \quad (3.3)$$

where e_s is the total static deflection of the shock strut and tire, and θ_{TD} is the pitch angle at touchdown. Note that the offset distance is dependent on the value of the pitch angle, whose value is similar to the pitch angle at liftoff, *i.e.*, between 12 and 15 degrees. For a low-wing passenger aircraft, h_{cg} can be approximated assuming a full load of passengers and no wing fuel [2]. This generally results in a vertical cg position at the main passenger-deck level.

3.3.2.2. Sideways Turnover Angle

Forces acting sideways on the airplane in cross-wind landing condition or a high-speed turn during taxiing could cause the aircraft to turnover on its side. It is thus desirable to keep the turnover angle (ψ) as small as possible. The angle is determined using the expression [2, p. 38]

$$\tan \psi = \frac{h_{cg}}{l_n \sin \delta} \quad (3.4)$$

where

$$\tan \delta = \frac{t}{2(l_m + l_n)} \quad (3.5)$$

and δ is defined as the angle between the aircraft centerline and the line connecting the center of the nose and main assembly. The dimensions used in the above equations are given in Fig. 3.3. For land-based aircraft, either the maximum allowable overturn angle of 63 degrees [2] or the stability considerations at takeoff and touchdown and during taxiing, whichever is the most critical, determines the lower limit for the track of the main assembly.

3.3.3. Braking and Steering Qualities

The nose assembly is located as far forward as possible to maximize the flotation and stability characteristics of the aircraft. However, a proper balance in terms of load distribution between the nose and main assembly must be maintained. When the load on the nose wheel is less than about eight percent of the maximum takeoff weight (MTOW), controllability on the ground will become marginal, particularly in cross-wind

conditions.* This value also allows for fuselage length increase with aircraft growth. On the other hand, when the static load on the nose wheel exceeds about 15 percent of the MTOW, braking quality will suffer, the dynamic braking load on the nose assembly may become excessive, and a greater effort may be required for steering [5]. Note that these figures should be looked upon as recommendations instead of requirements.

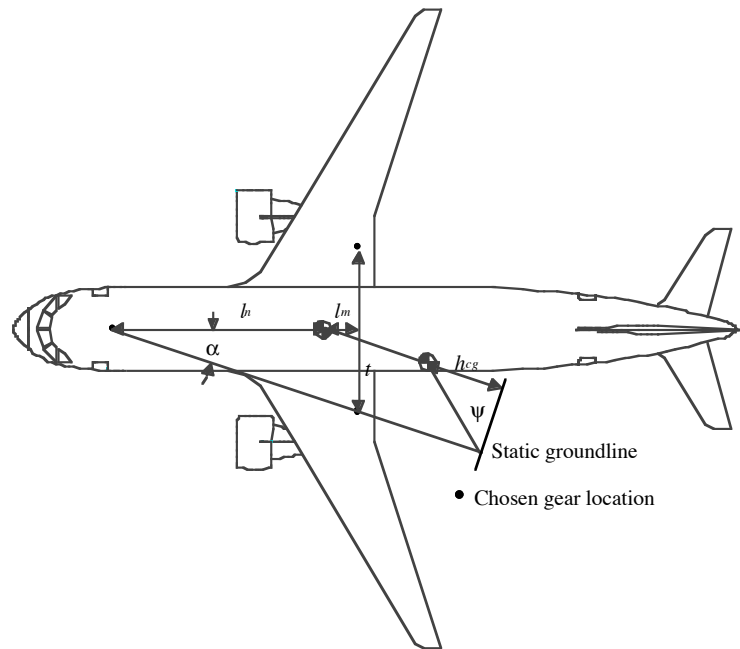


Figure 3.3 Turnover angle calculation [2]

3.3.4. Gear Length

Landing gear struts should be of sufficient length such that adequate clearance between the runway and all other parts of the aircraft, *e.g.*, the aft-body, wingtips, and engine nacelles, is maintained when the aircraft is on the ground. For a low-wing aircraft with wing-mounted engines, the above requirement proves to be one of the most challenging design issues in terms of permissible roll angle at touchdown. Although engine nacelle-to-ground clearance has not been explicitly defined, a similar requirement for propellers was specified in FAR Part 25 and can be used as an absolute minimum: a

* There are exceptions. The DC-9-50 has 3% on the nosewheel.

seven-inch clearance between the propellers and the ground in level takeoff or taxiing attitude, whichever is most critical. To date, the smallest offset on jet transports is found on the Boeing Model 747/GE90 testbed, where the GE90 engine nacelle clears the ground by a mere 13-inch clearance [21]. As for operational aircraft, the Boeing Model 737-300, -400, and -500 exhibit a 15-inch nacelle-to-ground clearance [22]. The length of the nose wheel strut is generally based on the requirement that the fuselage should be horizontal or tilted slightly nose-down when the aircraft is on the ground.

Besides the clearance considerations, allowance must also be considered for future stretching of the aircraft, which generally involves adding plugs forward and aft of the wing spars. Provided that the attitude of the aircraft will remain the same, the increase in the aft fuselage length would thus reduce the maximum permissible takeoff rotation angle, which can result in costly modifications and thus effectively rule out future growth options. Boeing abandoned further stretches of the Model 727 partially because of the difficulties encountered while attempting to maintain an adequate tail scrape angle, whereas Douglas was able to reduce the required tail scrape angle on the MD-11 by only structural changes, increasing the wing incidence by three degrees over that of its 22-foot shorter DC-10-30 forebear.

3.3.5. Landing Gear Attachment

From considerations of surrounding structure, the nose and main assembly are located such that the landing and ground loads can be transmitted most effectively, while at the same time still comply with the stability and controllability considerations. For a wing-mounted assembly, the trunnion is generally attached to the rear wing spar and the landing gear beam and the loads are transmitted directly to the primary wing-fuselage bulkheads. With the inclusion of fuselage-mounted assemblies in the multiple main-strut configurations, a secondary frame would then be added at a distance behind the rear wing-spar, where loads are transmitted forward to the primary wing-fuselage bulkhead through the keel and by shear in the fuselage skin. As for the nose assembly, structural considerations may be conclusive in deciding the mounting location, *i.e.*, at the proximity

of forward cabin bulkhead to minimize weight penalty due to local structural reinforcement.

3.4. Ground Operation Characteristics

Besides ground stability and controllability considerations, the high costs associated with airside infrastructure improvements, *e.g.*, runway and taxiway extensions and pavement reinforcements, have made airfield compatibility issues one of the primary considerations in the design of the landing gear [23]. In particular, the aircraft must be able to maneuver within a pre-defined space as it taxis between the runway and passenger terminal. For large aircraft, this requirement effectively places an upper limit on the dimension of the wheelbase and track.

3.4.1. Aircraft Turning Radii

As shown in Fig. 3.4, turning radii are defined as the distances between the center of rotation and various parts of the aircraft. The center of rotation is located at the intersection of the lines extending from the axes of the nose and main assemblies. For aircraft with more than two main struts, the line extending from the main assembly group is located midway between the fore and aft gears. The turning radii are a function of nose gear steering angle (β); the greater the angle, the smaller the radii. The upper limit for this angle is determined by the methods available to provide the steering action, which generally limits the angle to ± 60 degrees [2].*

The turning radius corresponding to an 180-degree turn ($r_{180^\circ \text{ turn}}$) as identified in Fig. 3.4 is determined using the expression

$$r_{180^\circ \text{ turn}} = t \tan(90 - \beta) + \frac{b}{2} \quad (3.6)$$

where b and t are the wheelbase and track, respectively. Given the aircraft design group classification as listed in Table Chapter 3 .1, the minimum turning diameter, *i.e.*, twice of

* This value may be low. The B737 has $\pm 75^\circ$, the DC-8 $\pm 74 \frac{1}{2}^\circ$, the DC-9 $\pm 80^\circ$, and the B767 $\pm 65^\circ$.

the 180-degree turn radius, should be less than the corresponding runway pavement width.

Table Chapter 3 .1 FAA airplane design group classification for geometric design for airports [7]

Airplane design group	Wingspan, ft	Runway width, ft
III	$79.0 < s < 118.0$	100.0
IV	$118.0 < s < 171.0$	150.0
V	$171.0 < s < 197.0$	150.0
VI	$197.0 < s < 262.0$	200.0

With the greater wheelbase and track dimensions as exhibited by large aircraft, the 180-degree turn maneuver can no longer be achieved with the conventional nose-steering scheme alone. As a result, combined nose and main assembly steering systems have been introduced on the newer large aircraft, *e.g.*, Boeing Models 747 and 777, to reduce the turning radii.* Other advantages provided by this feature include reduced tire wear and scuffing of the pavement surface in a sharp turn. Note that at the conceptual design phase of an aircraft, Eq. (3.6) is sufficient in producing a first-cut estimate. The resulting turning radii, which are based on nose-steering scheme, are slightly larger than the ones corresponding to combined nose and main assembly steering scheme, and thus provide a built-in safety margin.

* However, the first generation DC-8 also incorporated this feature.

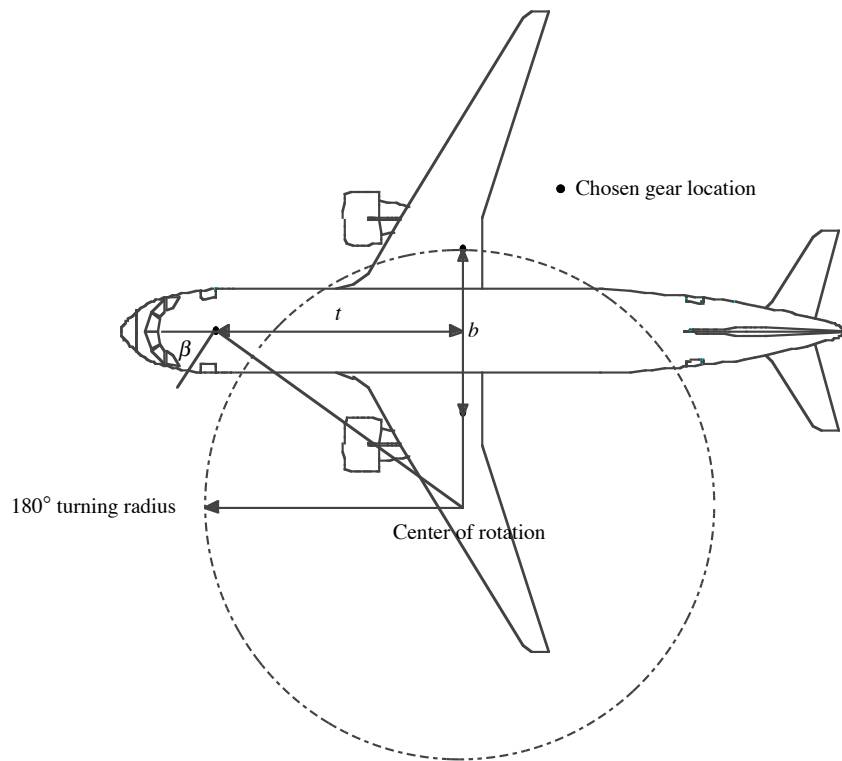


Figure 3.4 Aircraft turning radii [7]

3.4.2. Centerline-guidance Taxiing

The size of the fillets at runway and taxiway intersections depend not only on wheelbase, radius of centerline curve, width of taxiway, and total change in direction, but also on the path that the aircraft follows. There are two options in which an aircraft can be maneuvered on a turn: one is to establish the centerline of the taxiway as the path of the nose gear; the other is to assume that the nose gear follows a path offset outward of the centerline during the turn. The former is selected as the critical design case since it is the most demanding of the two in terms of piloting skill, *i.e.*, difficult to keep the nose wheel, which is below and behind the pilot's field of view, on the centerline while taxiing, and thus requires a greater area of pavement during the maneuver as safety margin.

As shown in Fig. 3.5, the maximum castor angle (φ), *i.e.*, the angle formed between the tangent to the centerline and the longitudinal axis of the aircraft, will occur at the end

of the turn, where the nose wheel is at the point of tangency. The angle is approximated by [7, p. 318]

$$\sin\varphi = \frac{b}{R} \quad (3.7)$$

where R is the radius of centerline curve. A re-check should be made at this point to make sure that the design castor angle is within the permissible range of the steering angle.

For a given wheelbase and track dimension, the required fillet radius (F) is calculated using the expression [5, p. 318]

$$F = \sqrt{R^2 + b^2 - 2Rb \sin\varphi} - \frac{t}{2} - S \quad (3.8)$$

where S is the minimum distance required between the edge of the outboard tire and the edge of the pavement. Given the aircraft design group classification number as determined from Table Chapter 3 .1 and the corresponding FAA design values as presented in Table Chapter 3 .2, the upper limit for the wheelbase and track of the aircraft can be determined using Eqs (3.7) and (3.8).

Table Chapter 3 .2 FAA recommended taxiway exit geometry [7]

	Group III	Group IV	Group V	Group VI
Centerline radius, ft	100.0	150.0	150.0	170.0
Fillet radius, ft	55.0	80.0	85	85.0
Safety margin, ft	10.0	15.0	15.0	20.0

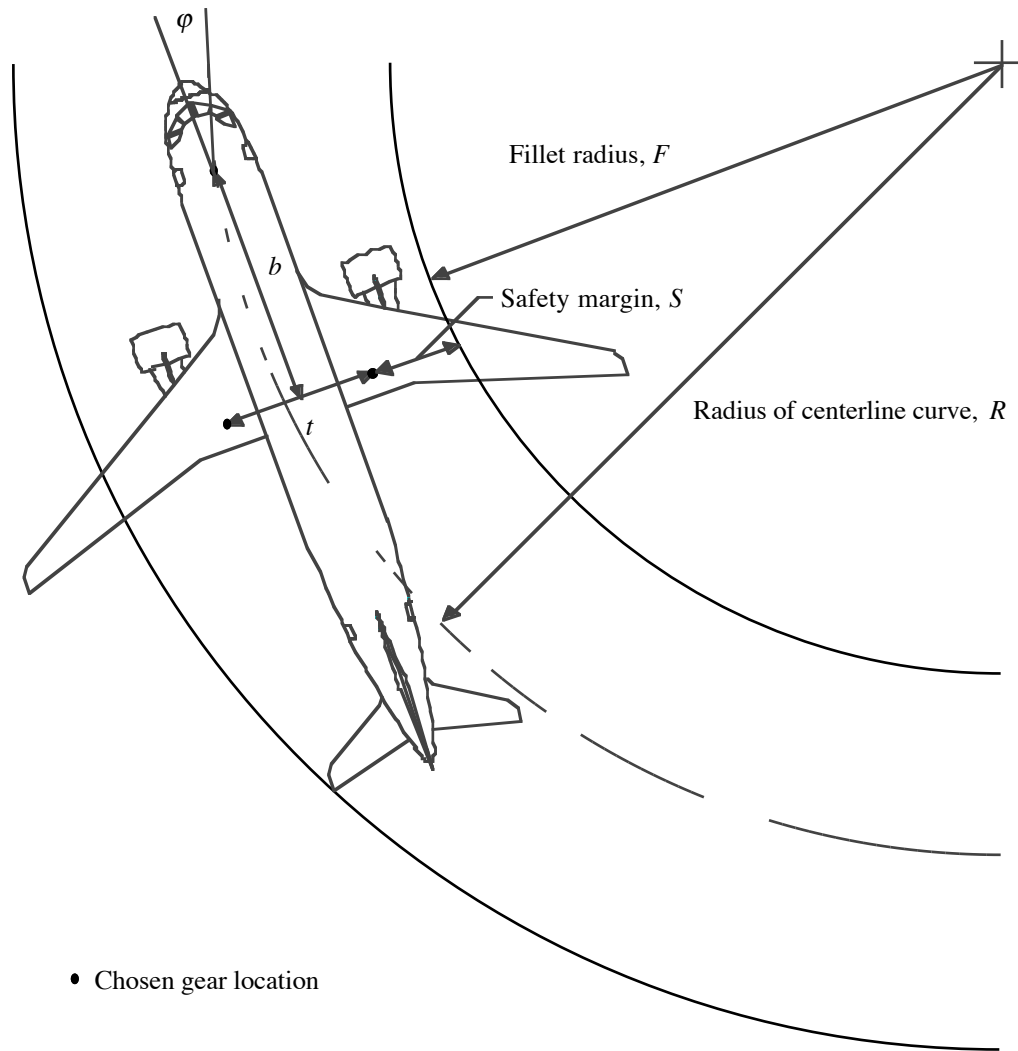


Figure 3.5 Taxiway fillet design [7]

3.5. Landing Gear Disposition Constraints

Landing gear location constraints as discussed in the above sections are superimposed on the three-view of a notional aircraft for illustrative purposes. As shown in Fig. 3.6a, the main assembly must be located such that when the shock strut is at the fully-extended position, the tire-ground contact point is below constraints II and IV in the vertical direction and outboard of constraint I in the lateral direction. In the top view as shown in Fig. 3.6b, the main assembly must also be located aft of constraint IV in the longitudinal direction and outboard of constraint V in the lateral direction. As for the nose assembly, it

must be located between constraints I and II in the longitudinal direction. And finally, as shown in Fig. 3.6c, the fully-extended tire-ground contact point is below constraint II in the vertical direction and aft of constraint II in the lateral direction.

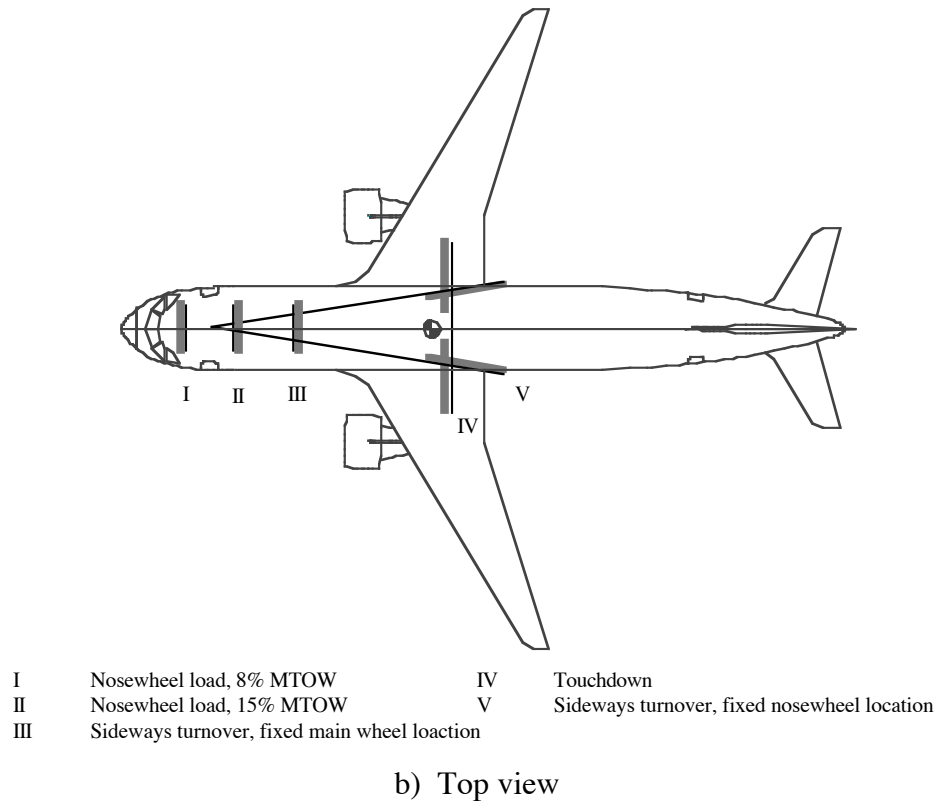
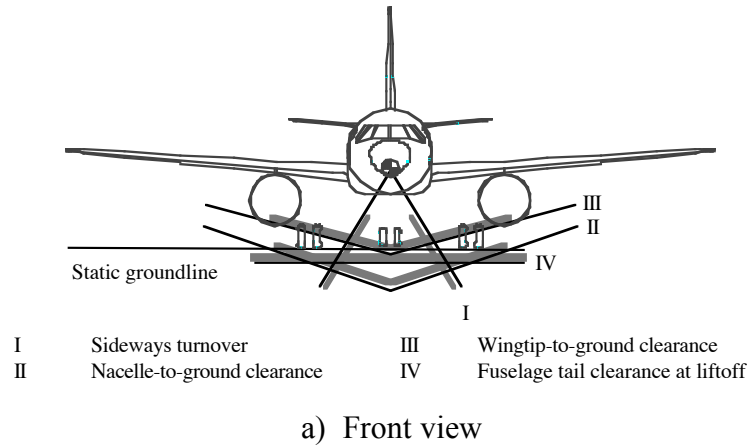
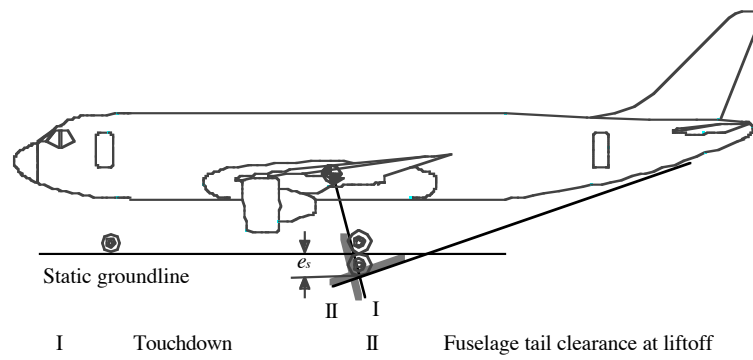


Figure 3.6 Landing gear attachment location constraints [5]



c) Side view

Figure 3.6 Landing gear attachment location constraints (cont'd)